



ARTICLE

Bilateral Filter for the Optimization of Composite Structures

Yuhang Huo¹, Ye Tian¹, Shiming Pu¹, Tielin Shi¹ and Qi Xia^{1,2,*}

¹State Key Laboratory of Digital Manufacturing Equipment and Technology, Huazhong University of Science and Technology, Wuhan, China

²State Key Laboratory of Structural Analysis for Industrial Equipment, Dalian University of Technology, Dalian, China

*Corresponding Author: Qi Xia. Email: qxia@mail.hust.edu.cn

Received: 06 January 2021 Accepted: 08 March 2021

ABSTRACT

In the present study, we propose to integrate the bilateral filter into the Shepard-interpolation-based method for the optimization of composite structures. The bilateral filter is used to avoid defects in the structure that may arise due to the gap/overlap of adjacent fiber tows or excessive curvature of fiber tows. According to the bilateral filter, sensitivities at design points in the filter area are smoothed by both domain filtering and range filtering. Then, the filtered sensitivities are used to update the design variables. Through several numerical examples, the effectiveness of the method was verified.

KEYWORDS

Design optimization; composite structure; fiber angle optimization; bilateral filtering; Shepard interpolation; manufacturability constraints

1 Introduction

Advanced manufacturing technologies of fiber-reinforced composite structures, for instance the automatic tape laying (ATL) and automatic fiber placement (AFP), allow composite structures to be manufactured with curvilinear fibers [1,2]. Therefore, stiffness can be different at different positions of the structure, and the freedom for improving the structural performance is larger than the constant stiffness composite structures [3–5]. However, the gap/overlap and excessive curvature of curvilinear fiber tows give rise to the appearance of manufacturing defects. The issue should be carefully dealt with at the design stage. When curvilinear fiber tows are not parallel [6–9], gaps and overlaps between adjacent fiber tows will appear. When the curvature of the fiber tow is too large, the tension and compression on the edges of the fiber tows will result in delamination and wrinkling [10,11].

How to avoid such defects has become an important topic in the design optimization of composite structures with curvilinear fibers, and many efforts have been made in recent years. Brampton et al. [8] employed the isolines of level set function to represent equally spaced fiber paths, hence preventing gaps/overlaps. Brooks et al. [11] treated fiber paths as the streamlines



of a vector field, and gaps/overlaps and curvatures are respectively controlled by the constraints of the curl and divergence of this vector field. Hao et al. [12] proposed a multi-stage design strategy based on lamination parameters, in which the curvature and parallelism constraints were formulated as inequalities by using path functions. Hong et al. [13] developed an approach that controls the curvature of a fiber path through the gradient of lamination parameters. Tian et al. [14] proposed a parametric divergence-free vector field (pDVF) method for the optimization of fiber angle arrangement, and it ensures that fibers in one-ply do not cross each other.

In our previous study, within the Shepard-interpolation-based framework for design optimization, a gap/overlap constraint and a curvature constraint were proposed [15]. However, the two constraints should be defined at each design point, thus there are a large number of constraints, and the optimization is not efficient. In order to enhance the optimization efficiency, in [16] two filters were proposed to address the issue of gap/overlap and excessive curvature. At each design point, the sensitivity is first filtered in a rectangular region around the point, and by this means the fiber curvature is controlled. Then, in another rectangular region around the point, the filtered sensitivities are averaged to ensure fibers parallel to each other. Finally, the resulting sensitivity information is used to update the design variable.

In the present study, we propose to integrate the bilateral filter into the Shepard-interpolation-based fiber angle optimization (SFAO) [17,18]. According to the bilateral filter, a circular area is defined at each design point, and sensitivities at design points in the circular area are smoothed by both domain filtering and range filtering. The domain filtering is responsible for smoothing the magnitude of sensitivities, and the range filtering is responsible for adaptively adjusting the strength of smoothing according to the difference of fiber angles. The filtered sensitivities are used to update the design variables. As compared to the two-filter approach in our previous study [16], the bilateral filter approach is simpler and more convenient. In addition, the bilateral filter developed for image processing [19–21] has also been applied to the SIMP (Solid Isotropic Material with Penalization) [22,23] method for structural topology optimization, and it was proved to be effective to suppress the checkerboard pattern and simultaneously obtain a high-contrast black-white pattern of structure.

2 Optimization Problem

In this paper, the minimum compliance problem defined in Eq. (1) is considered

find θ_i ($i = 1, 2, \dots, n$)

min $c = \mathbf{F}^T \mathbf{U}$

s.t. $\mathbf{K}\mathbf{U} = \mathbf{F}$

$\theta_{\min} \leq \theta_i \leq \theta_{\max}$ (1)

where θ_i is the fiber angle at the i -th design point; n is the total number of design points; c is the objective function, i.e., the compliance of the structure; \mathbf{F} is the global load vector; \mathbf{U} is the global displacement vector; \mathbf{K} is the global stiffness matrix; θ_{\max} and θ_{\min} are respectively the upper and lower bounds of the design variables, aiming to avoid the “ π -ambiguity” issue of fiber angles [18].

Inspired by Kang et al. [24,25], the Shepard interpolation was proposed in our previous study to describe the fiber angles in the design domain. The fiber angles at finite element centers are

computed by using a continuous function. This function is constructed by the Shepard method that interpolates the fiber angles at scattered design points, and it is given by [18]

$$\Theta(\mathbf{x}) = \sum_{i \in I_x} \omega_i(\mathbf{x}) \theta_i \tag{2}$$

where $\Theta(\mathbf{x})$ is the fiber angle at point \mathbf{x} ; I_x is the set of design points in the influence domain of point \mathbf{x} ; θ_i is the fiber angle at the design point at \mathbf{p}_i ; $\omega_i(\mathbf{x})$ is a weight function given by [26–28]

$$\omega_i(\mathbf{x}) = \frac{\|\mathbf{x} - \mathbf{p}_i\|^{-p}}{\sum_{i \in I_x} \|\mathbf{x} - \mathbf{p}_i\|^{-p}} \tag{3}$$

where $\|\mathbf{x} - \mathbf{p}_i\|$ is the Euclidean distance between point \mathbf{x} and design point \mathbf{p}_i ; p is a positive parameter, and in the present study $p = 2$ because this makes $\omega_i(\mathbf{x})$ infinitely differentiable [29]. This guarantees that the spatial variation of the fiber angle is continuous and smooth.

Another useful property of Shepard interpolation is expressed as

$$\min_i \{\theta_i\} \leq \Theta(\mathbf{x}) \leq \max_i \{\theta_i\} \tag{4}$$

According to Eq. (4), when the fiber angle at any point in the design domain needs to be constrained as $\Theta(\mathbf{x}) \in [\theta_{\min}, \theta_{\max}]$, this goal can be readily achieved by constraining the design variables θ_i as $\theta_i \in [\theta_{\min}, \theta_{\max}]$.

The equilibrium equation $\mathbf{K}\mathbf{U} = \mathbf{F}$ is solved by the finite element method. The global stiffness matrix \mathbf{K} is obtained by assembling the element stiffness matrix \mathbf{K}_e given by

$$\mathbf{K}_e = \int_{\Omega_e} \mathbf{B}^T \mathbf{D}(\theta_e) \mathbf{B} d\Omega \tag{5}$$

where \mathbf{B} is the displacement strain matrix; $\mathbf{D}(\theta_e)$ is the elastic matrix depending on the fiber angle (denoted as θ_e) in the e -th element, i.e.,

$$\mathbf{D}(\theta_e) = \mathbf{T}(\theta_e) \mathbf{D}_0 \mathbf{T}(\theta_e)^T \tag{6}$$

where \mathbf{D}_0 is the elastic matrix when the fiber is not rotated, and $\mathbf{T}(\theta_e)$ is the rotation matrix.

3 Sensitivity Analysis and Bilateral Filter

The sensitivity of the objective function with respect to design variables is given by [18]

$$\frac{\partial c}{\partial \theta_i} = - \sum_{e=1}^N \mathbf{u}_e^T \frac{\partial \mathbf{K}_e}{\partial \theta_e} \frac{\partial \theta_e}{\partial \theta_i} \mathbf{u}_e \tag{7}$$

The derivative of the fiber angle θ_e with respect to design variable θ_i is obtained through Eq. (2) as

$$\frac{\partial \theta_e}{\partial \theta_i} = \begin{cases} \omega_i(\mathbf{x}_e), & i \in I_{x_e} \\ 0, & i \notin I_{x_e} \end{cases} \tag{8}$$

where \mathbf{x}_e is the coordinate of the centroid of the e -th element; I_{x_e} is the set of design points in the influence domain of \mathbf{x}_e .

After the sensitivity of each design variable θ_i has been obtained according to Eq. (7), they are smoothed by the bilateral filter, as shown in Fig. 1. In order to improve the effects of filtering, the bilateral filter is usually applied to the sensitivities several times in each iteration of the optimization. The black dots represent the design points, and the yellow area is the bilateral filtering area. In this paper, the radius of the circular filtering area (denoted as r_{\min}) is 10 times the grid size of design points to include more design variables.

The bilateral filtering of sensitivities is written as

$$\frac{\widehat{\partial c}}{\partial \theta_i} = \frac{1}{H(\mathbf{p}_i)} \sum_{\mathbf{p}_j \in N_i} W_c(\|\mathbf{p}_j - \mathbf{p}_i\|) W_s(|\theta_j - \theta_i|) \frac{\partial c}{\partial \theta_j} \quad (9)$$

where N_i is the circular filtering area centered at the design point i ; $H(\mathbf{p}_i)$ is defined for normalization; $W_c(\|\mathbf{p}_j - \mathbf{p}_i\|)$ is the domain filtering function; $W_s(|\theta_j - \theta_i|)$ is the range filtering function. They are respectively given by [19,20]

$$H(\mathbf{p}_i) = \sum_{\mathbf{p}_j \in N_i} W_c(\|\mathbf{p}_j - \mathbf{p}_i\|) W_s(|\theta_j - \theta_i|) \quad (10)$$

$$W_c(\|\mathbf{p}_j - \mathbf{p}_i\|) = e^{-\frac{1}{2} \left(\frac{\|\mathbf{p}_j - \mathbf{p}_i\|}{\sigma_d} \right)^2} \quad (11)$$

$$W_s(|\theta_j - \theta_i|) = e^{-\frac{1}{2} \left(\frac{|\theta_j - \theta_i|}{\sigma_r} \right)^2} \quad (12)$$

where σ_d and σ_r are the parameters of domain filtering and range filtering respectively. The two parameters directly affect the performance of bilateral filtering [19,21]. σ_d controls the strengthen of Gaussian filtering, and σ_r controls the discrimination ability of fiber angles.

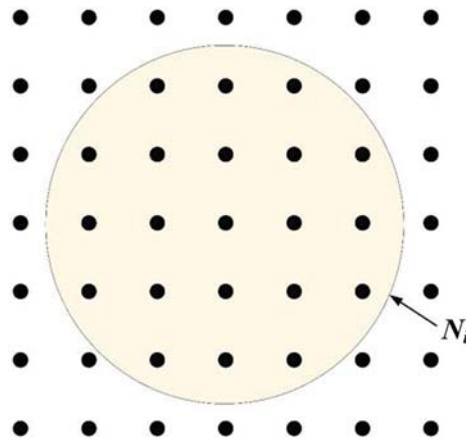


Figure 1: Schematic diagram of the sensitivity bilateral filtering area (the black dots represent the design points)

4 Numerical Examples

In this section, the proposed optimization method is applied to several 2D structures subjected to in-plane loads. In these examples, the mechanical properties of the composite material are assumed as $E_x = 1$, $E_y = 0.05$, $G_{xy} = 0.03$, $\nu_{xy} = 0.3$, $\nu_{yx} = 0.015$. Plane-stress quadrilateral elements are used for the finite element analysis, and self-weight of the structure is not considered. The criterion of convergence is that the number of iterations is no more than 50. According to our experience, 50 iterations are enough for convergence. When the initial value of the fiber angle is set as 0° , the upper and lower bounds of the design variables are set as $\theta_{\min} = -90^\circ$ and $\theta_{\max} = 90^\circ - \varepsilon$; ε is set as a very small value to avoid “ π -ambiguity” [18]. In this paper, ε is set as 1×10^{-8} . When the initial value of the fiber angles is set as 90° , the upper and lower limits of design variables are set as $\theta_{\min} = 0^\circ$ and $\theta_{\max} = 180^\circ - \varepsilon$.

The fiber angle distribution obtained by the optimization is post-processed by using the Tecplot software to generate fiber paths. In fluid dynamics, it is well known that the velocity of any point in a flow field is tangent to the streamline through the point. For the element e in the design domain, a vector at the element center is defined by

$$v_e = (\cos \theta_e, \sin \theta_e) \quad (13)$$

This vector is tangent to the fiber path through the element center. After importing the vector field constructed by Eq. (13), the Tecplot generates fiber paths.

4.1 Example 1

The first design problem is shown in Fig. 2. The size of the design domain is $1 \text{ m} \times 4 \text{ m}$. The lower-left corner is fixed, and the lower right corner is fixed vertically. The center of the top edge is subjected to a downward concentrated load F of 1 N. Because of the symmetry of the structure, only the right half is considered in the optimization.

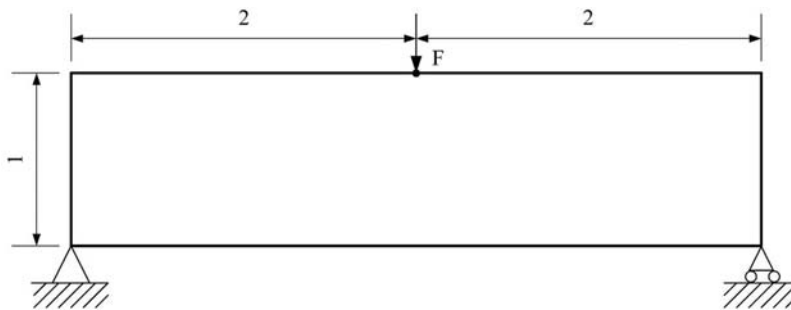


Figure 2: Design problem of the first example

Firstly, 10×20 design points are evenly arranged in the design domain. The initial value of θ_i at each design point is set as 0° , as shown in Fig. 3a. Then, the design domain is divided into 20×40 square elements. The initial fiber angles θ_e at the center points of all the elements are calculated by using the Shepard interpolation, as shown in Fig. 3b. The bilateral filter is applied to the sensitivities six times in each iteration of the optimization, and the parameters are set as $\sigma_r = 1$ and $\sigma_d = 5$. The results of optimization are shown in Fig. 4. The convergence history is shown in Fig. 5, and it can be seen that the optimization gradually converges after 20 steps.

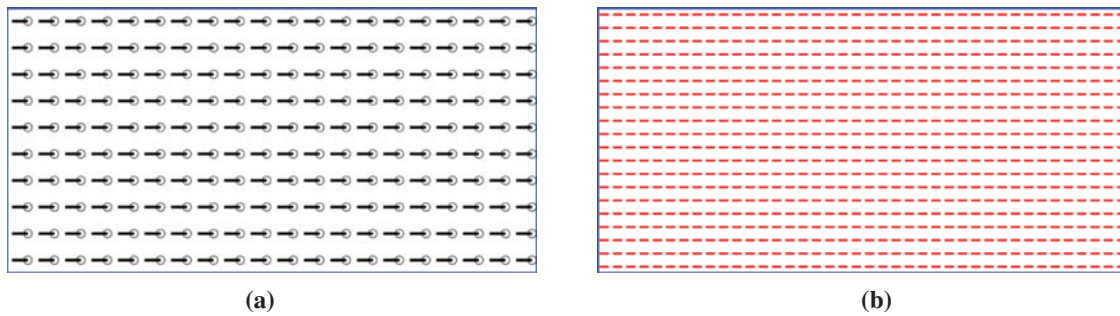


Figure 3: The initial arrangement of fiber angles for the first example. (a) Initial fiber angles at design points, (b) initial fiber angles at center points of finite elements

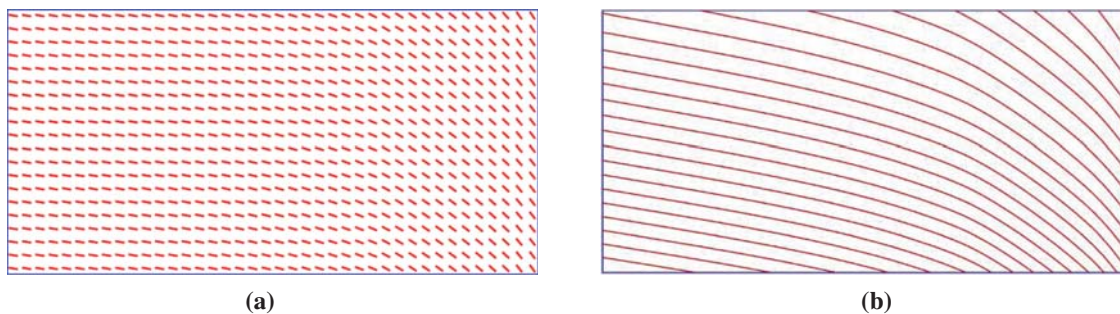


Figure 4: The results of the first example with $\sigma_r = 1$, $\sigma_d = 5$ and six repetitions of bilateral filtering in each iteration, and the structural compliance is 178.14. (a) The optimized fiber angles, (b) the fiber paths obtained by Tecplot

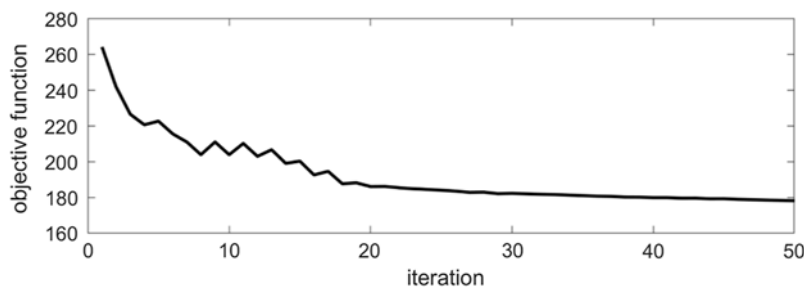


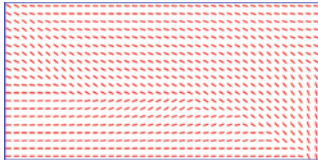
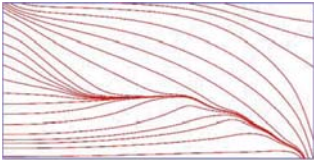
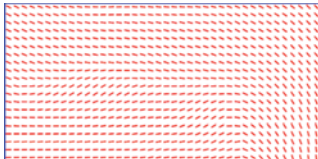
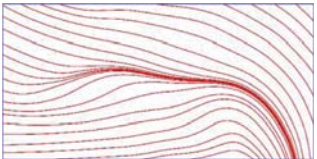
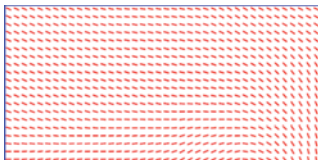
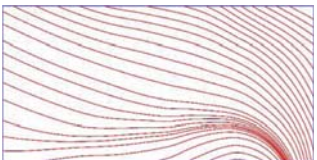
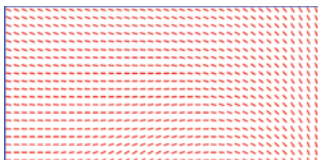
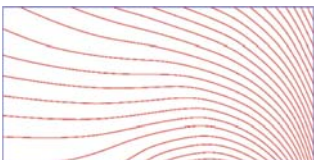
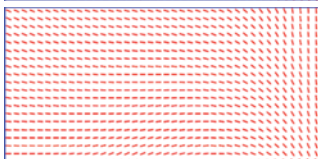
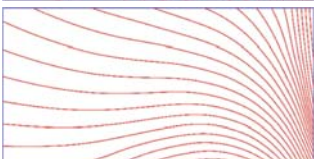
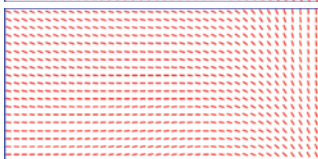
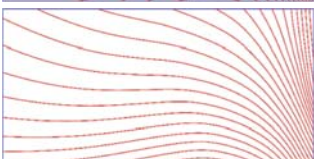
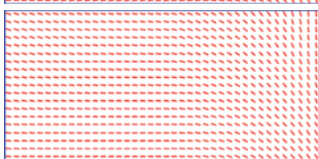
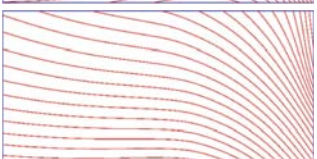
Figure 5: The convergence history of the first example

Next, we investigate the influence of the number of bilateral filtering on the optimization results. We will also analyze the influence of domain filtering parameter σ_d and range filtering parameter σ_r on the optimization results.

When the number of bilateral filtering in each iteration is investigated, the parameters are set as $\sigma_r = 1$ and $\sigma_d = 3$. The optimization results with different numbers of repetitions of bilateral filtering in each iteration are summarized in [Tab. 1](#). Without bilateral filtering, although the structural compliance can reach a smaller value of 72.39, severe overlaps of fibers can be found in the optimized structure, which does not meet the requirement of ATL or AFP manufacturing

technology, and such results have no practical use. With the increase of the number of bilateral filtering in each iteration, the distribution of fiber paths becomes more uniform, since the fiber paths are almost parallel and the curvature of fiber paths are smaller. These results proved that bilateral filtering is effective.

Table 1: The optimization results with different numbers of repetitions of bilateral filtering in each iteration (with fixed parameters $\sigma_r = 1$, $\sigma_d = 3$)

Filtering times	Fiber angles	Fiber paths	Compliance
0			72.39
1			95.09
2			105.84
4			116.90
5			116.47
6			116.26
8			138.98

Next, the influence of the domain filtering parameter σ_d and the range filtering parameter σ_r on the results are discussed. The number of repetitions of bilateral filtering in each iteration is set as six; the initial angle of the design point is set as 0° ; the results are shown in [Tabs. 2 and 3](#). It can be seen from [Tab. 2](#) that when σ_r is 0.1, the change of fiber angle is quite sharp; the fiber paths are not so smooth; the distance between fiber paths is not uniform. With the increase of σ_r , the spatial variation of the fiber angles becomes smoother. When σ_r increases from 3 to 5, the effect gradually weakens because the optimization results are almost the same. In addition, it can be seen from [Tab. 3](#) that the larger value of σ_d leads to significant smoothing of fiber angles [19,21]. Therefore, when the bilateral filter is used to optimize fiber angle, the parameters σ_r and σ_d need to be properly set. According to our experience gained from numerical examples, we suggest that σ_r should be selected between 0.5~2 and σ_d should be selected between 3~5.

Table 2: The optimization results obtained with different σ_r

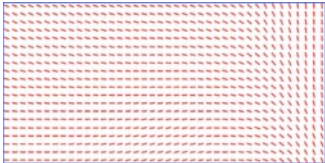
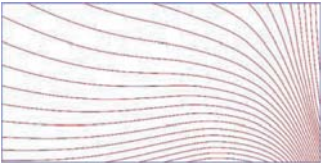
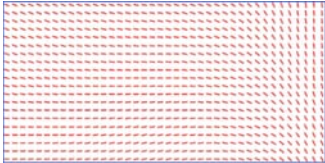
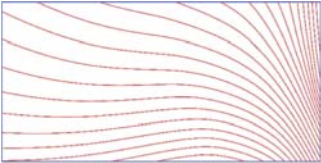
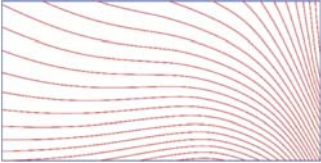
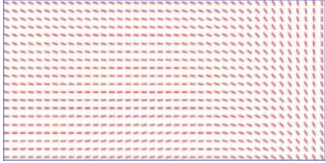
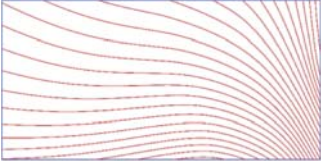
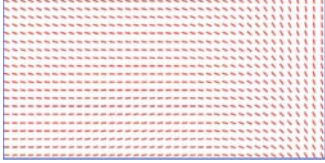
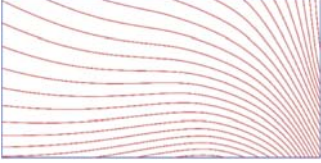
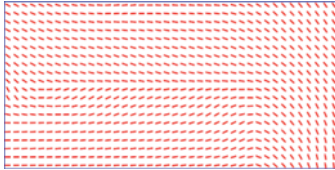
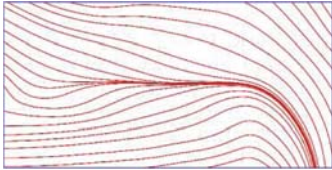
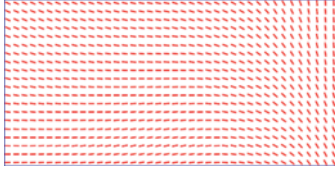
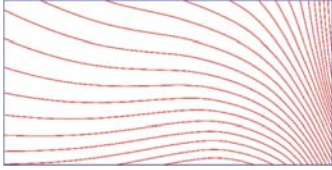
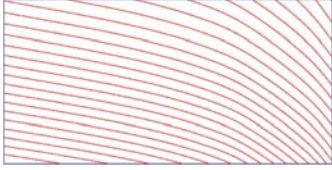
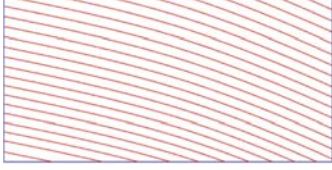
Parameters		Fiber angles	Fiber paths	Compliance
σ_d	σ_r			
3	0.1			134.83
3	0.5			111.44
3	1			116.26
3	2			117.97
3	3			117.87
3	5			118.04

Table 3: The optimization results obtained with different σ_d

Parameters		Fiber angles	Fiber paths	Compliance
σ_d	σ_r			
1	1			90.13
3	1			116.26
5	1			178.14
8	1			216.39

4.2 Example 2

The second design problem is shown in Fig. 6. The design domain is 1 m × 3 m in size, fixed at the left edge. Also, it is subjected to in-plane load F of 1N, and evenly distributed along the boundary at the top right with a width of 0.5 m. In the design domain, there are 10 × 30 design points uniformly arranged, and the initial values of all the θ_i are 0°, as shown in Fig. 7a. The design domain is divided into 20 × 60 square elements. The initial fiber angle θ_e at the center points of all the elements are calculated by the Shepard interpolation, and they are shown in Fig. 7b. The bilateral filter is applied to the sensitivities six times in each iteration of optimization, and the parameters are set as $\sigma_r = 1$ and $\sigma_d = 5$. The results of the second example are shown in Fig. 8.

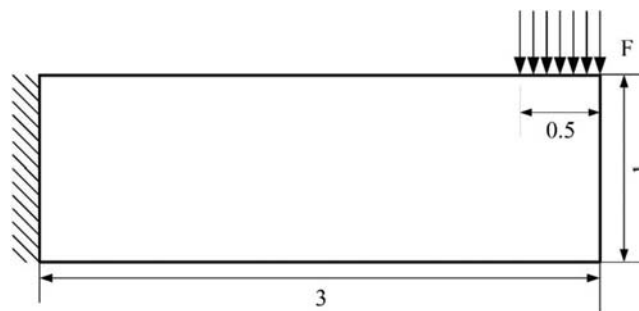


Figure 6: Design problem of the second example

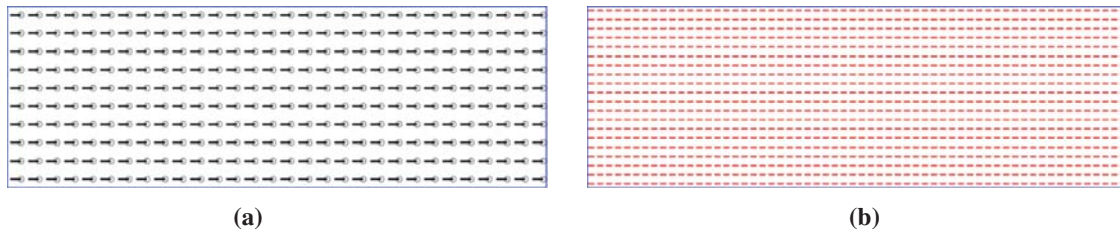


Figure 7: The initial arrangement of fiber angles for the second example. (a) Initial fiber angles at design points, (b) initial fiber angles at center points of finite elements

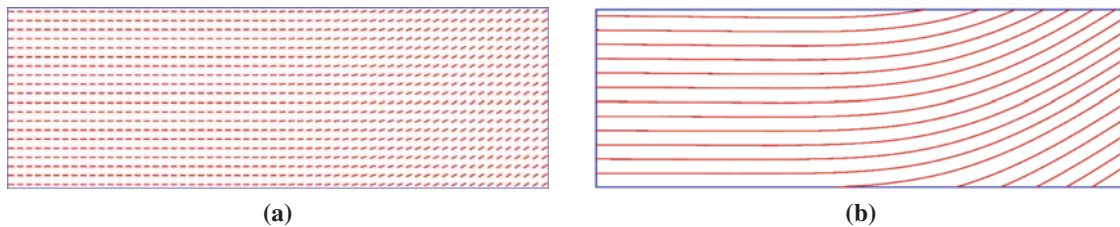


Figure 8: The results of the second example with $\sigma_r = 1$, $\sigma_d = 5$ and six repetitions of bilateral filtering in each iteration, and the structural compliance is 195.63. (a) The optimized fiber angles, (b) the fiber paths obtained by Tecplot

It can be seen from Fig. 8b that the fiber paths are almost parallel to each other, which means that there exists no gap or overlap between adjacent fiber tows. In addition, the fiber paths are fairly smooth, which means that their curvatures are not large. At the same time, the optimization results also show that the suggested values of the parameters for the bilateral filter in the first example are reasonable.

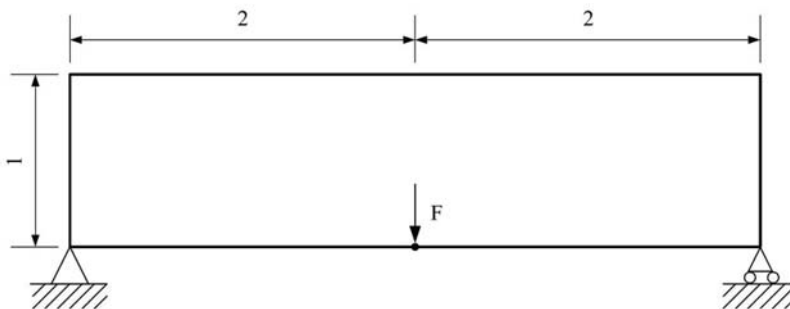


Figure 9: Design problem of the third example

4.3 Example 3

The third design problem is shown in Fig. 9. The design domain is $1 \text{ m} \times 4 \text{ m}$ in size. The lower-left corner is fixed and the lower right corner is fixed vertically. The concentrated load F of 1 N is applied at the middle point of the bottom edge. There are 10×40 design points uniformly arranged in the design domain, and the initial value of θ_i at all the design points are 0° , as shown in Fig. 10a. The design domain is divided into 20×80 square elements. The initial fiber angle

θ_e at the center points of all the elements are shown in Fig. 7b. The bilateral filter is applied to the sensitivities four times in each iteration, and the parameters are set as $\sigma_r = 1$ and $\sigma_d = 5$. The results are shown in Fig. 11. Through this example, the effectiveness of bilateral filtering in fiber angle optimization is proved again. As can be seen in Fig. 11b, the fiber paths are parallel, equidistant, and without large curvature.

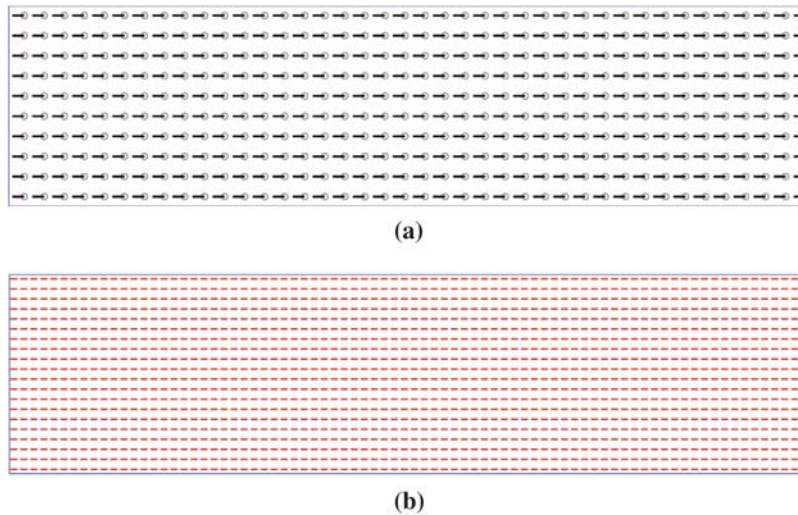


Figure 10: The initial arrangement of fiber angles for the third example. (a) Initial fiber angles at design points, (b) initial fiber angles at center points of finite elements

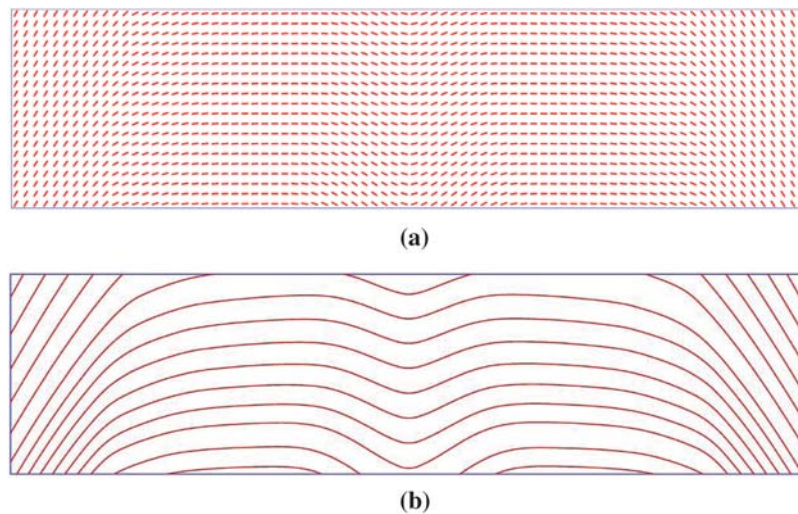


Figure 11: The optimization results of the third example with $\sigma_r = 1$, $\sigma_d = 5$ and four repetitions of bilateral filtering in each iteration, and the structural compliance is 82.05. (a) The optimized fiber angles, (b) the fiber paths obtained by Tecplot

5 Conclusions

In this paper, the bilateral filter was integrated into the Shepard-interpolation-based method for the optimization of composite structures. According to the bilateral filter, sensitivities at design points in the filter area are smoothed by both domain filtering and range filtering. Then, the filtered sensitivities are used to update the design variables. Through several numerical examples, it was found out that the bilateral filter is useful to avoid gap/overlap between adjacent fiber tows or excessive curvature of fiber tows.

Funding Statement: This research work was supported by the National Natural Science Foundation of China (Grant No. 51975227) and the Natural Science Foundation for Distinguished Young Scholars of Hubei Province, China (Grant No. 2017CFA044).

Conflicts of Interest: The authors declare that they have no conflicts of interest to report regarding the present study.

References

1. Xu, Y. J., Zhu, J. H., Wu, Z., Cao, Y. F., Zhao, Y. B. et al. (2018). A review on the design of laminated composite structures: Constant and variable stiffness design and topology optimization. *Advanced Composites and Hybrid Materials*, 1(3), 460–477. DOI 10.1007/s42114-018-0032-7.
2. Nikbakt, S., Kamarian, S., Shakeri, M. (2018). A review on optimization of composite structures Part I: Laminated composites. *Composite Structures*, 195(1), 158–185. DOI 10.1016/j.compstruct.2018.03.063.
3. Ghiasi, H., Pasini, D., Lessard, L. (2009). Optimum stacking sequence design of composite materials Part I: Constant stiffness design. *Composite Structures*, 90(1), 1–11. DOI 10.1016/j.compstruct.2009.01.006.
4. Ghiasi, H., Fayazbakhsh, K., Pasini, D., Lessard, L. (2010). Optimum stacking sequence design of composite materials Part II: Variable stiffness design. *Composite Structures*, 93(1), 1–13. DOI 10.1016/j.compstruct.2010.06.001.
5. Dirk, H. L., Ward, C., Potter, K. D. (2012). The engineering aspects of automated prepreg layup: History, present and future. *Composites Part B*, 43, 997–1009. DOI 10.1016/j.compositesb.2011.12.003.
6. Tatting, B. F., Gürdal, Z., Jegley, D. (2002). *Design and manufacture of elastically tailored tow placed plates*.
7. Wu, K., Tatting, B., Smith, B., Stevens, R., Occhipinti, G. et al. (2009). Design and manufacturing of tow-steered composite shells using fiber placement. *50th AIAA/ASME/ASCE/AHS/ASC Structures, Structural Dynamics, and Materials Conference*. California: Palm Springs.
8. Brampton, C. J., Wu, K. C., Kim, H. A. (2015). New optimization method for steered fiber composites using the level set method. *Structural and Multidisciplinary Optimization*, 52(3), 493–505. DOI 10.1007/s00158-015-1256-6.
9. Bruyneel, M., Zein, S. (2013). A modified fast marching method for defining fiber placement trajectories over meshes. *Computers and Structures*, 125(2), 45–52. DOI 10.1016/j.compstruc.2013.04.015.
10. Lozano, G. G., Tiwari, A., Turner, C., Astwood, S. (2016). A review on design for manufacture of variable stiffness composite laminates. *Proceedings of the Institution of Mechanical Engineers, Part B: Journal of Engineering Manufacture*, 230(6), 981–992. DOI 10.1177/0954405415600012.
11. Brooks, T. R., Martins, J. R. (2018). On manufacturing constraints for tow-steered composite design optimization. *Composite Structures*, 204(3), 548–559. DOI 10.1016/j.compstruct.2018.07.100.
12. Hao, P., Liu, D. C., Wang, Y., Liu, X. X., Wang, B. et al. (2019). Design of manufacturable fiber path for variable-stiffness panels based on lamination parameters. *Composite Structures*, 219(2), 158–169. DOI 10.1016/j.compstruct.2019.03.075.
13. Hong, Z., Peeters, D., Turteltaub, S. (2020). An enhanced curvature-constrained design method for manufacturable variable stiffness composite laminates. *Computers and Structures*, 238(C), 106284. DOI 10.1016/j.compstruc.2020.106284.

14. Tian, Y., Pu, S. M., Shi, T. L., Xia, Q. (2021). A parametric divergence-free vector field method for the optimization of composite structures with curvilinear fibers. *Computer Methods in Applied Mechanics and Engineering*, 373(14), 113–574. DOI 10.1016/j.cma.2020.113574.
15. Tian, Y., Pu, S. M., Zong, Z. H., Shi, T. L., Xia, Q. (2019). Optimization of variable stiffness laminates with gap-overlap and curvature constraints. *Composite Structures*, 230(6), 111–494. DOI 10.1016/j.compstruct.2019.111494.
16. Tian, Y., Huo, Y. H., Shi, T. L., Xia, Q. (2021). Filters for manufacturability in design optimization of variable stiffness composites. *Chinese Journal of Aeronautics*, 34(4), 153–159. DOI 10.1016/j.cja.2020.07.028.
17. Tian, Y., Mou, J. X., Shi, T. L., Xia, Q. (2019). Shepard interpolation based on geodesic distance for optimization of fiber reinforced composite structures with non-convex shape. *Applied Composite Materials*, 26(2), 575–590. DOI 10.1007/s10443-018-9731-z.
18. Xia, Q., Shi, T. L. (2018). A cascadic multilevel optimization algorithm for the design of composite structures with curvilinear fiber based on Shepard interpolation. *Composite Structures*, 188(2014), 209–219. DOI 10.1016/j.compstruct.2018.01.013.
19. Tomasi, C., Manduchi, R. (1998). Bilateral filtering for gray and color images. *Proceedings of the 1998 IEEE International Conference on Computer Vision*, pp. 839–846. Bombay, India.
20. Michael, Y. W., Wang, S. Y. (2005). Bilateral filtering for structural topology optimization. *International Journal for Numerical Methods in Engineering*, 63(13), 1911–1938. DOI 10.1002/nme.1347.
21. Jiang, W., Baker, M. L., Wu, Q., Bajaj, C., Chiu, W. (2003). Applications of a bilateral denoising filter in biological electron microscopy. *Journal of Structural Biology*, 144(1), 114–122. DOI 10.1016/j.jsb.2003.09.028.
22. Zhou, M., Rozvany, G. I. N. (1991). The COC algorithm. Part II: Topological, geometrical and generalized shape optimization. *Computer Methods in Applied Mechanics and Engineering*, 89(1–3), 309–336. DOI 10.1016/0045-7825(91)90046-9.
23. Bendsoe, M. P., Sigmund, O. (1999). Material interpolation schemes in topology optimization. *Archive of Applied Mechanics*, 69(9–10), 635–654. DOI 10.1007/s004190050248.
24. Kang, Z., Wang, Y. Q. (2012). A nodal variable method of structural topology optimization based on Shepard interpolant. *International Journal for Numerical Methods in Engineering*, 90(3), 329–342. DOI 10.1002/nme.3321.
25. Kang, Z., Wang, Y. Q. (2011). Structural topology optimization based on non-local Shepard interpolation of density field. *Computer Methods in Applied Mechanics and Engineering*, 200(49), 3515–3525. DOI 10.1016/j.cma.2011.09.001.
26. Shepard, D. (1968). A two-dimensional interpolation function for irregularly-spaced data. *Proceedings of the 23rd National Conference*, pp. 517–523. New York, USA: ACM.
27. Brodlie, K., Asim, M., Unsworth, K. (2005). Constrained visualization using the Shepard interpolation family. *Computer Graphics Forum*, 24(4), 809–820. DOI 10.1111/j.1467-8659.2005.00903.x.
28. Lodha, S. K., Franke, R. (1997). Scattered data techniques for surfaces. *Scientific Visualization Conference*, pp. 189–230. Dagstuhl, Germany.
29. Farwig, R. (1986). Rate of convergence of Shepard's global interpolation formula. *American Mathematical Society*, 46, 577–590. DOI 10.1090/S0025-5718-1986-0829627-0.